# AUTOMATIC SEGMENTATION OF PULMONARY VASCULATURE IN THORACIC CT SCANS WITH LOCAL THRESHOLDING AND AIRWAY WALL REMOVAL

*Evelien van Dongen[1], Bram van Ginneken[1,2]*

1) Image Sciences Institute, University Medical Center Utrecht, The Netherlands
2) Diagnostic Image Analysis Group, Department of Radiology, Radboud University Nijmegen Medical Centre, The Netherlands

## ABSTRACT

*A system for the automatic segmentation of the pulmonary vasculature in thoracic CT scans is presented. The method is based on a vesselness filter and includes a local thresholding procedure to accurately segment vessels of varying diameters. The output of an automatic segmentation of the airways is used to remove false positive detections in the airway walls. The algorithm is tested with a quantitative evaluation framework based on manual classification of well-dispersed local maxima and random points on ten axial sections in a scan. The algorithm has been applied to ten low dose CT scans annotated by two observers. Results show that local thresholding and airway wall removal both improve segmentation performance and that the accuracy of the proposed method approaches the interobserver variability.*

***Index Terms —*** *Pulmonary image analysis, computed tomography, vessel segmentation, vessel enhancement, airway wall removal, optimal thresholding.*

## 1. INTRODUCTION

The automatic segmentation of the pulmonary vasculature is an essential preprocessing step for many algorithms that analyze thoracic CT scans. An accurate segmentation can be used to exclude the vessels from further analysis, for instance to improve nodule detection algorithms. Also, the vessel tree segmentation itself can be used for the detection of pulmonary embolisms and for quantification of hypertension in which the diameter of the arteries provide an indicator for cardiovascular risk.

Many vessel segmentation algorithms are based on the detection of tubular structures by computing features from the eigenvalues of the Hessian matrix [1-3]. A different class of segmentation algorithms uses wavefront propagation or another type of tracking to grow the vessel tree from a number of initial seed points [2, 4-6]. Although most of these algorithms take shape features into account, effective suppression of noise and high density structures such as airways walls, fissures, and abnormalities remains an important issue.

The evaluation of algorithms to segment the pulmonary vessel tree in CT scans is a complicated task. Producing a complete and reliable reference standard for the highly complicated and intertwined vascular trees in the lungs is prohibitive. As a result, most previously proposed segmentation algorithms have not been extensively evaluated. Current methods include the (aided) manual segmentation or manual extraction of centerlines of complete CT scans on a number of sections [3-5] and the manual placement of points in the vessels [2]. Also, experts have visually assessed the correctness of the segmentation [6]. However, many algorithms have only been evaluated qualitatively by the algorithm developers [1, 7].

In this work we propose a segmentation algorithm based on Frangi's vesselness filter [1] in which local optimal thresholding is applied around the centerlines and in which the airway walls are explicitly excluded from the segmentation. The second major contribution of this work is the introduction of a novel evaluation framework for the quantitative analysis of vessel segmentation algorithms.

## 2. SEGMENTATION METHOD

The proposed segmentation method consists of five steps, which are discussed in the following subsections.

### 2.1. Lung segmentation and airway wall removal (AR)

For the segmentation of the vessel tree only the lung areas require examination. Lung segmentation is based on the hybrid algorithm by Van Rikxoort et al. [8]. The resulting lung segmentation is eroded with a spherical structuring element (SE) with a half size of 3 voxels to prevent voxels on the border of the lungs to be classified as vessel.

A wavefront propagation algorithm by Van Ginneken et al. [9] is used to automatically segment the airways. The resulting airway segmentation only provides the airway lumen. To exclude the airway walls from further computations it is assumed that the thickness of the walls is around 2 mm; airway walls are excluded by dilating the

airway segmentation with a spherical SE with a radius of 3 voxels.

### 2.2. Vessel enhancement

Vessels are enhanced by computing the vesselness based on a slightly modified version of the multi-scale filter by Frangi et al. [1]. The eigenvalues of the Hessian matrix are determined at different scales $\sigma$. Lindeberg's $\gamma$-normalization [10] is applied to normalize the response over different scales in order to facilitate scale selection. $\gamma$ is set to 1.0 to achieve scale invariance. The vesselness $V_{max}$ is computed as a probability based on the following ratios between the eigenvalues, with $|\lambda_1| \leq |\lambda_2| \leq |\lambda_3|$:

$$R_b = \frac{|\lambda_1|}{\sqrt{(|\lambda_2\lambda_3|)}} \quad , \quad R_a = \frac{|\lambda_2|}{|\lambda_3|} \quad , \quad S = \sqrt{{\lambda_2}^2 + {\lambda_3}^2}.$$

These terms are combined into the following probability formula:

$$V_0(\sigma) = \begin{cases} 0 & if\ I(x,y,z) < -750\ or\ \lambda_2 > 0\ or\ \lambda_3 > 0 \\ \left(1 - exp\left(-\frac{{R_a}^2}{2\alpha^2}\right)\right) exp\left(-\frac{{R_b}^2}{2\beta^2}\right)\left(1 - exp\left(-\frac{S^2}{2c^2}\right)\right), \end{cases}$$

where $\alpha$, $\beta$ and $c$ are parameters that control the sensitivity of the ratios, set at 0.5, 0.5, and 70, respectively. The vesselness is evaluated at 7 different scales varying from the voxel size in mm up to 4.5 mm, exponentially distributed. The vesselness, $V_{max}(x)$, is defined as the maximum response over all scales; $\sigma_{max}(x)$ is the scale at which the vesselness response is maximal. $\sigma_{max}$ provides an estimation of the width of the vessel. The direction of the vessel is determined by $e_1(x)$, the eigenvector corresponding to $\lambda_1(x)$.

Vessel segmentation methods described in literature often use a similar vessel enhancing filter. To create a final segmentation, the output of the filter can be thresholded. Although these filters are good in detecting the vessels, they are often not accurate enough to provide a good segmentation. The next subsections describe a method that uses additional information to create a more accurate segmentation. To put that method into perspective, it is compared to a thresholded vesselness output image, which will be referred to as $VT_t$, with threshold $t$.

### 2.3. Multi-scale thresholding

Due to the partial volume effect, smaller pulmonary vessels have a lower density on CT, which results in a lower vesselness. A single threshold on the vesselness does therefore not provide a satisfactory segmentation. To correct for this, a multi-scale threshold is used with lower thresholds for voxels that correspond to small vessels and thus have a small $\sigma_{max}$.

$$V(V_{max,}\sigma_{max}) = \begin{cases} 0, & V_{max} < T(\sigma_{max}) \\ 1, & V_{max} \geq T(\sigma_{max}) \end{cases}$$

$$T(\sigma_{max}) = \begin{cases} T_{min}\, exp\left(\frac{i\, ln\,(T_{max}/T_{min})}{n-1}\right), & \sigma_{max} < w \\ T_{max}, & \sigma_{max} \geq w \end{cases}$$

where $n$ is the number of scales smaller than $w$, which is set to 2 times the voxel size in mm; $i$ is the index of the scale, with $i = 0,...,n$. $T_{min}$ was set to 0.07 and $T_{max}$ to 0.17.

### 2.4. Centerline extraction

The thinning algorithm by Palagyí et al. [11] is used to delete non-centerline voxels. This mask-based algorithm iteratively removes 'simple points', defined as those points whose removal does not change the topology of the object, until no further voxels can be removed.

### 2.5. Local optimal thresholding (LT)

Each centerline voxel is assigned a type based on the number of neighboring voxels $n$: segment ($n=2$), bifurcation ($n>2$), endpoint ($n=1$). If $n=0$ the voxel is discarded. Endpoint voxels connected to a bifurcation voxel are also discarded, to remove small trailing centerlines. Segment voxels are grouped together if connected. This process results in groups of centerline voxels that each form a part of the vessel tree, with $k$ voxels each.

Next, a segmentation is created from the centerline voxels by applying local optimal thresholding [12]. For this, a local region of interest (roi) is defined around each group of centerline voxels as is shown in Figure 1. The shape of the roi is chosen such that it resembles the shape of the vessel tree part: cylindrical for groups of segment voxels and spherical for bifurcation and endpoint voxels. The radii $r_{cyl}$, $r_{sphere}$ of the shapes are determined by $\sigma_{max}$ in mm:

$$r_{cyl} = 1.5 \max_{0 \leq i \leq k} (\sigma_{max}(x_i), 3),\ r_{sphere} = 1.5 \max_{0 \leq i \leq k} (\sigma_{max}(x_i), 4),$$

The direction of the cylindrical roi is determined by the direction of the vessel by taking the average over all $e_1(x_i)$, with $i = 0,..,k$. Because these direction vectors might not be consistent throughout the whole group of segment voxels, the groups are first cut up into smaller pieces of connected voxels with an overlap between each piece as is illustrated in Figure 1. A cylindrical roi is then created for each small segment. For each roi, the optimal threshold is determined and then applied by region growing from the centerline while a minimal required vesselness of 0.05 is taken into account to prevent the algorithm from leaking into other high density structures.

The method that uses local thresholding is indicated as LT. The final method we propose also excludes the airway walls and is indicated as LT + AR.

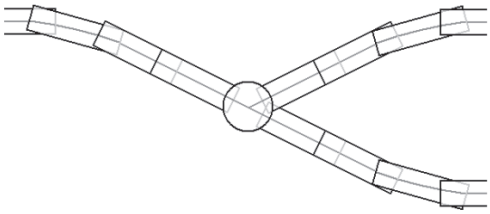

Figure 1: Schematic drawing of the construction of regions of interest around centerlines.

## 3. EVALUATION FRAMEWORK

The evaluation framework required trained experts to label a set of points in axial sections of the lungs as vessel or non-vessel. The latter category was further subdivided into airway wall, fissure, abnormality or other. These points were generated by taking local maxima in 2D in the axial sections, after blurring with a Gaussian kernel with a scale of 1.0 mm to reduce spurious responses. Only maxima with a density above -750 HU were considered. Because most points selected in this way are vessels, 30% random points were added per section. To prevent clusters of points, a minimum distance of 10 voxels between each pair of points was required. In order to limit the number of points that experts should label, only 10 sections, equally distributed over the scan in the z-direction, were used. The evaluation framework limits the time required for evaluation, because points are generated automatically. This also results in the unbiased evaluation of small as well as large vessels.

## 4. RESULTS

Experiments have been performed with 10 low dose ($CTDI_{vol} \approx 1$ mSv) scans from 16-slice scanners or higher with sub-millimeter near isotropic resolution from a lung cancer screening program from asymptomatic subjects, scanned at full inspiration. In these scans, a total of 7376 points were classified by two observers. The classifications of the first observer were used as the reference standard.

For each of these scans, segmentations were created with 4 methods. These methods were compared to the second observer. Table 1 provides confusion matrices of the results for all segmentation methods and the second observer, as well as sensitivity and specificity.

To check the performance of the algorithm for vessels of different widths, the points were also sorted by intensity and divided into categories, with the assumption that points with a lower intensity belong to smaller vessels. This showed that for the proposed method almost 61% of the false negatives resulted from points with an intensity between -800 and -700 HU. An additional 35% of the false negatives belonged to points with an intensity between -700 and -600 HU. This resulted in a low sensitivity for points between -1000 up to -600 HU of only 0.52.

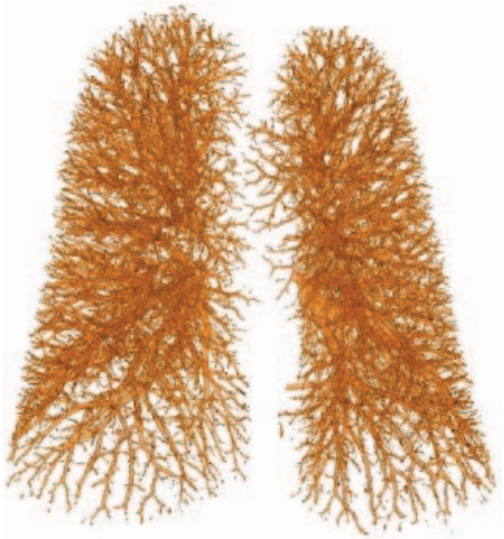

Figure 2: Volume rendering of segmented vasculature using the proposed LT + AR algorithm for one of the test scans.

The effect of the explicit airway wall removal was evaluated by a further analysis of the false positives. The false positives were divided into the different non-vessel categories, with an exception for abnormalities. Table 2 shows the percentage of false positives as part of all points within that specific category. After airway wall removal, the percentage of false positives in the airway wall category as part of the total number of points, indicated in the reference standard as belonging to the airway wall, approached the interobserver variability. This percentage is clearly lower than that of $VT_{0.07}$ and LT.

| | | **$VT_{0.07}$** | | **$VT_{0.15}$** | | **LT** | | **LT + AR** | | **2nd observer** | |
|---|---|---|---|---|---|---|---|---|---|---|---|
| | | Y | N | Y | N | Y | N | Y | N | Y | N |
| **ref** | Y | 3291 | 1534 | 2088 | 2737 | 3426 | 1399 | 3419 | 1406 | 4142 | 683 |
| | N | 171 | 2380 | 50 | 2501 | 184 | 2367 | 145 | 2406 | 133 | 2418 |
| sensitivity | | 0.68 | | 0.43 | | 0.71 | | 0.71 | | 0.86 | |
| specificity | | 0.93 | | 0.98 | | 0.93 | | 0.94 | | 0.95 | |

Table 1: Total performance over all scans for 4 different segmentation methods and the second human observer with observer 1 as reference standard. Y indicates a vessel classification; N corresponds to a non-vessel classification.

| | $VT_{0.07}$ | $VT_{0.15}$ | LT | LT + AR | 2nd |
|---|---|---|---|---|---|
| Other | 3.9 | 0.06 | 4.1 | 4.1 | 4.8 |
| **Airway** | **34.9** | **15.4** | **39.1** | **16.0** | **11.2** |
| Fissure | 17.1 | 7.9 | 18.6 | 18.6 | 3.6 |

Table 2: Percentage of false positives per category over the total number of points in these categories for each of the four methods and for the second observer.

## 5. DISCUSSION AND CONCLUSION

The results show that the proposed LT + AR algorithm produces better results than direct thresholding of the vesselness output and that the removal of airway walls improves performance slightly. When comparing LT to $VT_{0.07}$, sensitivity is increased without compromising the specificity. This is due to the multi-scale thresholding and local optimal thresholding, which decrease the number of false negatives. Adding airway wall removal further improves the results by decreasing the number of false positives. Because of the relatively low amount of evaluation points on the airway walls, the improvement of the overall results is limited. However, it should be noted that, when tracing the vascular tree to analyze for instance connectivity, false responses on airway walls cause substantial problems, because they create false connections between separate vessels. By removing these false positives, connectivity becomes more reliable, which is essential for further analysis of the intertwined arterial and venous vessel trees in the lungs.

Results from direct thresholding of the vesselness show that the vesselness filter is in itself not sufficient to distinguish between vessels and airway walls. With a threshold of 0.07, almost 35% of the points on the airways walls are misclassified as vessels. A higher threshold obviously reduces the number of false positives, but at the cost of a substantial decrease in sensitivity, as can be seen from the results of $VT_{0.15}$.

Even a fairly simple airway wall exclusion method, as is described in this paper, is able to reduce the number of false positives in the category of airway wall points from around 39% to 16%. It can be expected that a more sophisticated airway wall segmentation will further decrease the number of false positives.

The specificity of the segmentation algorithm is similar to the interobserver specificity. Sensitivity is lower due to the smaller vessels to which the vesselness is not very sensitive, which can be seen from the performance of the algorithm for points between -1000 and -600 HU. This illustrates that the partial volume effect decreases the vesselness of the smaller vessels, because of the smaller eigenvalues due to less contrast. For the detection of small vessels the vesselness filter might have to be improved.

Finally, it should be taken into account that the observers, although trained with the same data, disagree about the classification of 11% of all points, of which most correspond to small vessels. This shows that a reliable assessment of small vessels is a difficult task even for trained human observers.

Further research should prove whether the performance of the segmentation method is also high for a larger amount of scans, including scans with pathology.

## 6. REFERENCES


[1] A. Frangi, W.J. Niessen, K.L. Vincken, M.A. Viergever: Multiscale vessel enhancement filtering. In: MICCAI, LNCS, vol. 1496, pp. 130-137 (1998)

[2] H. Shikata, E.A. Hoffman, M. Sonka: Automated Segmentation of Pulmonary Vascular Tree from 3D CT Images. In: Proc. SPIE, vol. 5369, pp 107-116 (2004)

[3] G. Agam, S.G. Armato, C. Wu: Vessel tree reconstruction in thoracic CT scans with application to nodule detection. IEEE Transactions on Medical Imaging, vol. 24, no. 4, pp. 486-499 (2005)

[4] O. Wink, W.J. Niessen, B. Verdonck, M.A. Viergever: Vessel axis determination using wave front propagation analysis. In: MICCAI, LNCS, vol. 2208, pp.845-853 (2001)

[5] T. Bülow, C. Lorenz, S. Renisch: A general framework for tree segmentation and reconstruction from medical volume data. In: MICCAI, LNCS, vol. 3216, pp. 533-540 (2004)

[6] M.A. Gülsün, H. Tek: Robust vessel tree modeling. In: MICCAI, LNCS, vol. 5241, pp.219-226 (2008)

[7] T. Bülow, R. Wiemker, T. Blaffert, C. Lorenz, S. Renisch: Automatic extraction of the pulmonary artery tree from multi-slice CT data. In: Proc. SPIE, vol. 5746, pp. 730-740 (2005)

[8] E.M. van Rikxoort, B. de Hoop, M.A. Viergever, M. Prokop, B. van Ginneken: Automatic lung segmentation from thoracic computed tomography scans using a hybrid approach with error detection. Medical Physics, vol. 36, pp. 2934-2947 (2009)

[9] B. van Ginneken, W. Baggerman, E.M. van Rikxoort: Robust segmentation and anatomical labeling of the airway tree from thoracic CT scans. In: MICCAI, LNCS, vol. 5241, pp. 219-226 (2008)

[10] T. Lindeberg: Edge detection and ridge detection with automatic scale selection. In: Proc. CVPR, pp. 465-470 (1996)

[11] K. Palagyí, A. Kuba: A 3D 6-subiteration thinning algorithm for extracting medial lines. Pattern Recognition Letters, vol. 19, pp. 613-627 (1998)

[12] W. Ridler, S. Calvard: Picture thresholding using an iterative selection method. IEEE Transactions on Systems, Man, and Cybernetics, vol. SMC-8, pp. 630-632 (1978)